Systematic Jitter in a Chain of Digital Regenerators

By C. J. BYRNE,* B. J. KARAFIN and D. B. ROBINSON, JR.

(Manuscript received May 29, 1963)

Digital pattern variations are a major source of timing jitter in self-timed digital regenerators. In a chain of similar regenerators, the same jitter is introduced at each one. Therefore, the jitter accumulates systematically.

A model is introduced to predict the accumulation of jitter in a chain of identical regenerators with single tuned timing filters. Simple expressions have been derived from the model for the response of the timing phase to sudden pattern transitions and to random patterns. These results show that the jitter grows without bound in a long chain, but its form is such that the tendency to cause errors will not increase as the chain becomes longer.

Measurements on a chain of 84 regenerators in a field installation are in excellent agreement with the theory.

I. INTRODUCTION

An ideal digital regenerator must restore the shape and timing of a received signal. A self-timed regenerator extracts the timing information from the received pulse train by means of a narrow bandpass filter tuned to the repetition rate. Imperfections in the regenerator and noise in the channel disturb the timing information and cause the phase of the pulse train to vary. This variation is called jitter.

Jitter in self-timed repeaters has been studied for some time. Sunde[1] and DeLange[2] concluded that jitter due to random noise would not be serious. Attention then turned to jitter introduced in the timing tanks by pattern variations. Bennett[3] studied a single mistuned regenerator. Rowe[3] analyzed a long chain of tuned regenerators. S. O. Rice studied jitter due to a random pattern in a long chain of systematically detuned regenerators.

The first fully developed digital regenerator intended for use in long chains became available in 1961. This was the repeater for the T1 PCM

* Bellcomm, Inc.

Carrier System. Investigations of jitter in this repeater by R. C. Chapman, Jr. and later by the present authors clearly indicated that the predominant jitter in chains was caused by systematic sources related to the pattern. No one cause of jitter was predominant, but rather several contributed significantly. Mistuning did not appear to be a major contributor.

As a result of these observations, it was felt that a simple, approximate theory was needed instead of the more complex, precise attack which had been used with mistuning. Should each of the several sources of jitter require its own precise analysis, the complete analysis, with all sources, might be extremely cumbersome. Therefore, Chapman proposed a simple model which depends on measurement to give the phase shift generated in each repeater. He used the model to predict how jitter would build up in a long chain of repeaters for a transition from one repetitive pattern to another. In this paper we will adopt Chapman's model and derive from it the behavior of a long chain of repeaters for arbitrary input patterns. The theory derives the dynamic behavior of a long chain of repeaters from static measurements of a short chain of repeaters using simple repetitive patterns.

The theory has been tested by measurements on a chain of 84 repeaters, installed in the field. Agreement with the theory is very good, and is best for the repeaters near the end of the chain. There is no theoretical reason or experimental evidence to suspect that the theory is not valid for much longer chains.

II. A MODEL OF JITTER ACCUMULATION

In a self-timed forward acting regenerator[5] (see Fig. 1) a timing wave is extracted from the received digital signal by a narrow bandpass filter. This timing wave will be phase modulated by whatever jitter has accumulated in the signal. The filter will smooth or reduce the amount of the phase modulation.

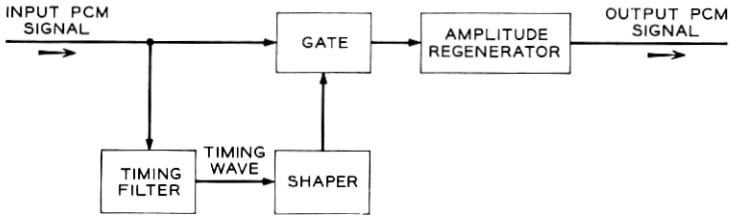

Fig. 1 — Block diagram of a self-timed forward acting regenerator.

The filtered timing wave is then used to retime the digital pattern. With ideal retiming a sharp spike is formed. This spike determines the time at which a decision is made by the amplitude regenerator and thus determines the leading edge of each pulse. Therefore, the digital pattern carries the phase of the timing wave as pulse position information. Some high-frequency, fine structure is lost, since only digital marks carry timing information, but the high-frequency jitter is not significant in long chains.

In the process of extracting, reshaping, and using the timing wave, the regenerators distort the timing and inject jitter. This jitter adds to that in the incoming signal and is processed with it in all regenerators further down the chain. The total jitter tends to increase as the chain grows longer. Our purpose is to describe the manner in which this jitter accumulates.

The model originally proposed by Chapman is shown in Fig. 2. The digital signal is not represented, since it acts only as a carrier for the timing wave for present purposes. The delays between regenerators are also eliminated, since they do not affect the manner of jitter accumulation.

A number of assumptions have been made to make the model tractable. These are:

1. The same jitter is injected at each repeater. This assumption precludes causes such as random noise and neglects variations in regenerator parameters. This assumption seems reasonable, since systematic jitter accumulates more rapidly than the nonsystematic type, and therefore the jitter at the end of a sufficiently long chain will be predominantly due to systematic causes. The most likely sources of systematic jitter are those which are related to the digital pattern itself, which is the same at each regenerator.

2. All significant jitter sources can be represented by an equivalent

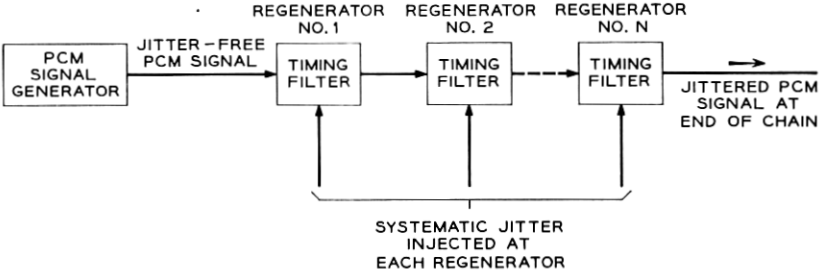

Fig. 2 — Block diagram of Chapman's model for jitter accumulation.

jitter at the input of each timing tank. This apparently arbitrary assumption will be discussed in the section on jitter sources.

3. Jitter adds linearly from repeater to repeater.

4. The timing tank is a simple single-tuned circuit, tuned to the pulse repetition frequency.

5. If the rate of change of phase jitter is small, then, as shown in Appendix A, as far as phase modulation is concerned, the timing tank is equivalent to a single-pole low-pass filter. The pole corresponds to the half bandwidth of the tuned circuit.

Therefore,

$$\Theta_o = \frac{1}{1 + (s/B)} \Theta_i \tag{1}$$

where

θ_i is the input jitter
θ_o is the output jitter
$B = \omega_o/2Q$ is the half bandwidth of the tank.

Inspection of (1) shows that very low-frequency jitter is unchanged by the timing filter, while higher-frequency jitter is attenuated and phase shifted.

The jitter introduced in the first repeater will be modified by the jitter transfer function of the timing filter and passed on to the second repeater. Here the same jitter will be introduced again and added to the jitter received from the first. The sum will be operated on by the timing tank of the second repeater and the result passed on to the third. This sequence will be repeated to the end of the chain, accumulating jitter all the way.

The jitter at the end of a chain of N repeaters will be equal to the sum of the jitter introduced in the last repeater operated on by one tank, the jitter introduced in the next-to-last repeater operated on by two tanks in cascade, and so on back to the first repeater. Since the jitter waveforms introduced in each repeater are assumed to be identical, we can express the sum as

$$\Theta_N(s) = \sum_{n=1}^{N} \Theta(s) \left(\frac{1}{1 + (s/B)}\right)^n \tag{2}$$

where $\Theta(s)$ is the transform of the pattern jitter introduced at each repeater.

The right-hand side of (2) is the sum of a geometric series and can easily be shown to be

$$\Theta_N(s) = \Theta(s)\,\frac{B}{s}\left[1 - \left(\frac{1}{1 + (s/B)}\right)^N\right]. \tag{3}$$

Equation (3) has an interesting approximation. If we neglect short-time (high-frequency) phenomena, we can restrict our attention to the region where the magnitude of s is much less than B. Then for large N,

$$\left(\frac{1}{1 + (s/B)}\right)^N \approx \exp\left(-N\,\frac{s}{B}\right). \tag{4}$$

Substituting this into (3) we have

$$\Theta_N(s) \approx \Theta(s)\,\frac{B}{s}\left[1 - \exp\left(-\frac{N}{B}\,s\right)\right]. \tag{5}$$

In the time domain, (5) becomes

$$\theta_N(t) \approx B\left[\int_{-\infty}^{t} \theta(t)\,dt - \int_{-\infty}^{t} \theta\left(t - \frac{N}{B}\right) dt\right] \tag{6}$$

$$\theta_N(t) \approx B\int_{t-(N/B)}^{t} \theta(t)\,dt. \tag{7}$$

Random jitter is more suitably represented by its power density than its Laplace transform. The term "power" is misleading here, because the square of an angle has no relation to power. However, we can define angular power density in direct analogy to a voltage power density: the angular power density at a frequency f is the mean squared value of the spectral components of the angle in a band one cycle per second wide centered at f.

The power density of jitter at the end of a chain of N repeaters can be found by replacing s by $j\omega$ in (3) and finding the square of the magnitude of the transfer function;

$$\Phi_N = \left(\frac{B}{\omega}\right)^2 \left|1 - \left(\frac{1}{1 + j(\omega/B)}\right)^N\right|^2 \Phi \tag{8}$$

where Φ is the power density of the jitter injected in each repeater.

A simpler approximation to (8) can be derived from (5)

$$\Phi_N \approx N^2\left[\frac{\sin\dfrac{N}{2B}\,\omega}{\dfrac{N}{2B}\,\omega}\right]^2 \Phi. \tag{9}$$

The exact transfer function given in (8) has been computed and is plotted in Fig. 3 for a range of values of N (the number of repeaters in the chain). At very low frequencies the transfer function is flat, and the power gain is proportional to the square of N. For higher frequencies, the power gain falls off as the inverse square of frequency. As a result of this spectrum shaping, the bulk of the jitter gain for large N is at low frequency. The strong ripples are interesting, but of little practical significance.

We will return to a study of the properties of (3) and (8), but first we will study the sources of jitter in each repeater.

III. SOURCES OF JITTER

Systematic jitter must be caused by a disturbance which arrives at successive regenerators in step with the pattern. The most likely cause of such a disturbance is variation in the pattern itself. In an ideal regenerator the pattern would have no effect on the phase of the timing wave. Unfortunately, in actual repeaters there are many imperfections which produce phase variations correlated with the pattern.

Causes of pattern jitter include intersymbol interference, finite pulse width effects, amplitude-to-phase conversion, and mistuning of the timing filter. These sources are extremely difficult to analyze in detail; furthermore, a careful analysis of one regenerator design would have to be completely redone for another.

As we shall show, the complexity of these jitter sources occurs principally in the detailed high-frequency fine structure of the jitter. The low-frequency behavior of jitter (averaged over many pulses) is much more tractable. In fact, the low-frequency jitter due to an arbitrary pulse pattern can be predicted from measurements with a small set of test signals. This permits us to completely ignore the detailed analysis of the jitter sources, using very simple measurements of a few sample regenerators instead.

The methods that will be used in this section lack rigor and the assumptions are not fully justified. This situation cannot be remedied without doing just what we wish to avoid: performing exhaustive analysis of a particular repeater design. Therefore, we proceed without rigor and rely on the experimental evidence to validate the results.

The first step is to show that the major sources of jitter can be represented by an equivalent jitter introduced before the timing filter, and that this jitter at a particular instant depends only on the last few bits of the pattern. In other words, there are no long memory mechanisms in the equivalent jitter sources.

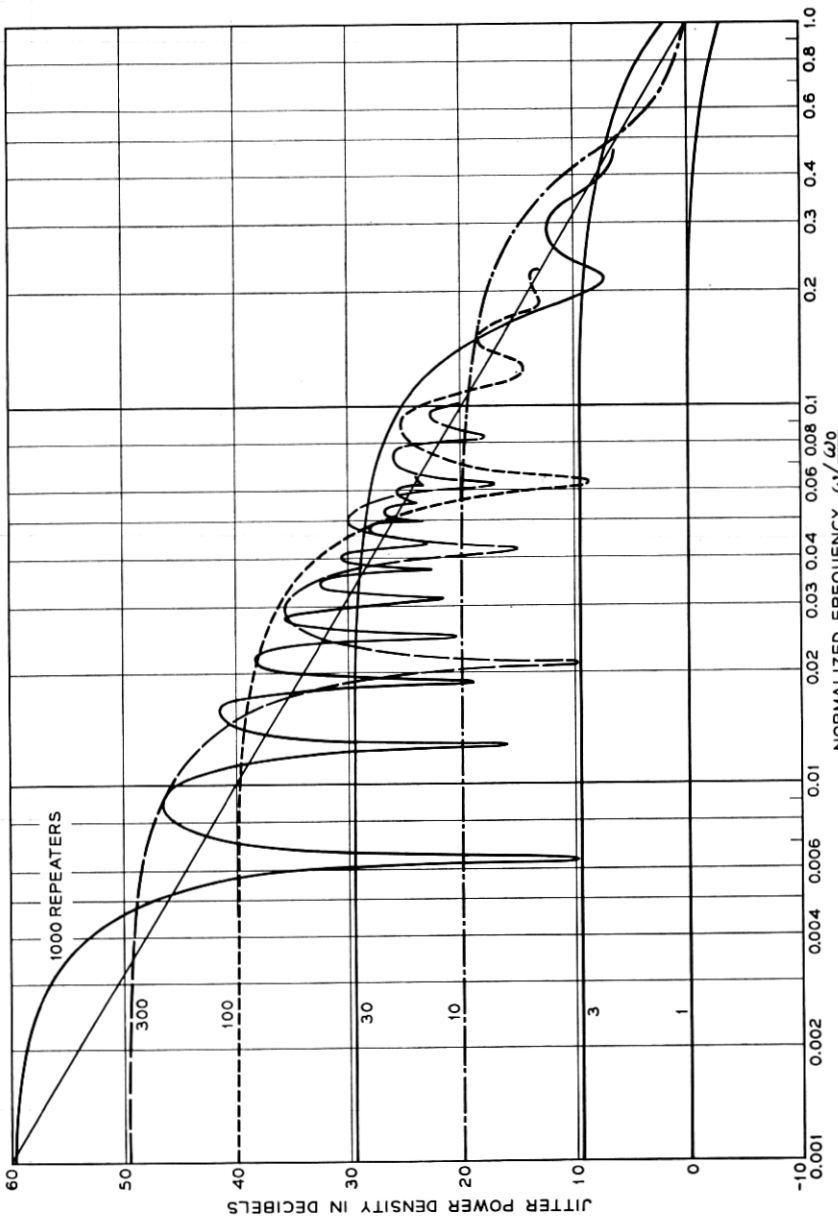

Fig. 3 — Jitter spectrum due to a random pattern (computed from the model).

The first source to be considered is intersymbol interference. Imperfect equalization of the transmission transfer function results in smearing each pulse so that adjacent pulses overlap to some extent. When clipping is used to reduce noise, the effective center of a pulse depends on whether or not pulses are adjacent to it. This effect occurs in front of the timing filter and the interaction of the pulses is effective over only a few bit intervals. Therefore, interpulse interference has the properties we assumed for jitter sources.

Finite pulse width effects[4] and amplitude-to-phase conversion are similar in that they both depend upon the amplitude of the timing wave in the tank circuit. This amplitude varies with the density of the pattern. Finite pulse width effects are due to the disturbance of the timing wave when a pulse is actually present. The amount of the phase disturbance depends upon the amplitude of the timing wave. Amplitude-to-phase conversion occurs in detecting zero crossings of the timing wave in order to form spikes for ideal retiming. If the threshold is not exactly at the zero level of the timing wave, a phase shift will be introduced which depends upon the timing wave amplitude.

At first sight, the jitter due to the timing wave amplitude variations appears to contradict the assumptions about jitter sources, since the variations are in a signal which has been operated on by the timing filter. However, we can show that these effects are equivalent to phase shifts before the filter.

The digital bit pattern can be regarded as a high-frequency amplitude modulation of a carrier at the bit repetition frequency. This signal, which is also phase modulated by jitter, is passed through the timing filter. It is shown in Appendix A that the output of the timing filter (the timing wave) will be amplitude and phase modulated, and if $A_i(s)$ is the transform of the input amplitude modulating signal, and if this signal is small, then

$$A_o(s) = A_i(s) \frac{1}{1 + (s/B)} \tag{10}$$

where $A_o(s)$ is the transform of the timing wave amplitude modulating signal and B is the half bandwidth of the timing filter.

If there is an amplitude-to-phase conversion mechanism with a coefficient C, the timing wave jitter will be

$$\Theta_o(s) = CA_o(s) = CA_i(s) \frac{1}{1 + (s/B)}. \tag{11}$$

But it is also shown in Appendix A that a phase modulation $\Theta(s)$ be-

fore the filter will cause a timing wave modulation given by

$$\Theta_o(s) = \Theta_i(s) \frac{1}{1 + (s/B)}. \tag{12}$$

By comparing (11) with (12) it can be seen that a jitter source operating on the amplitude modulation of the timing wave after the filter can be replaced by an equivalent jitter source operating on the amplitude modulation of the bit pattern before the filter. The equivalent jitter source is given by

$$\Theta_i(s) = CA_i(s). \tag{13}$$

Note that there are no long-term repeater memory effects in this jitter. Thus the timing wave amplitude sources have the properties we assumed.

The remaining source of jitter is mistuning of the timing filter. No simple argument can be presented to show that a proper equivalent exists for this. However, S. O. Rice has made a careful study of the systematic mistuning jitter. He has found that such jitter is equal to the sum of two terms: a high-frequency term which is predominant for short chains, and a low-frequency term which is predominant for long chains. The latter term is identical to the result we obtain using our model. Therefore, although mistuning does not directly fit our model, the results for this special source agree with those predicted by our model. In the case of the particular regenerators used in the experiments reported below, mistuning did not appear to be a major source of jitter.

As we have said, the above demonstration is not absolutely rigorous, and in the end we depend on the experimental evidence to justify our assumptions. This demonstration shows, however, that the model is not without some theoretical justification. So now, considering that all the important jitter sources can be represented by equivalent sources in front of the timing filter and that there are no long-term repeater memory mechanisms associated with these equivalent sources, we proceed to show how the jitter caused by an arbitrary bit pattern can be predicted from measurements with a set of test signals.

A sample from a bit sequence is shown in Fig. 4(a). Consider this as a sequence of blocks of 8 bits each. The factors involved in choosing a block length of 8 will be discussed later. The jitter introduced during the time span of a particular block will be chiefly caused by the bits within the block and only slightly influenced by bits outside of the block. This is a consequence of the assumption that there are no long memory mechanisms involved.

Therefore, it is reasonable to assign a particular value to the phase shift

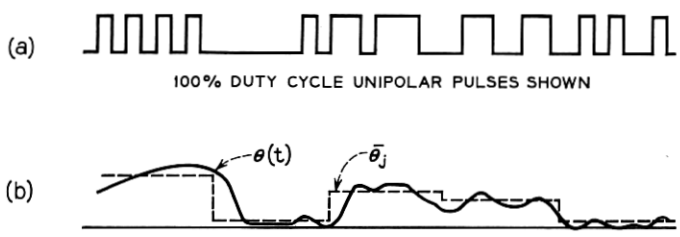

Fig. 4 — (a) Sample from a bit sequence; (b) actual and approximate jitter waveforms.

of each 8-bit block. This value is the average value of the actual phase shift over the interval. The resultant approximate jitter waveform is shown in Fig. 4(b).

The average value of phase shift for a particular 8-bit block may be determined by repeating the block over and over again with a suitable test signal generator and measuring the dc phase shift that results. By this means, an average phase shift $\bar{\theta}_j$ can be measured for each possible pattern j. There are 36 patterns 8 bits long which are distinct when repeated. These patterns are shown in Table I.

The block length used for measurement must be a compromise; it should be as long as possible to minimize end effects, but if it is too long there will be so many distinct patterns that the measurements would be impractical. The length 8 was chosen as a reasonable value.

We are now able to represent the jitter $\theta(t)$ injected due to an arbitrary pattern in terms of measurements with a few test signals. The resultant representation is not valid for high frequencies because of the artificial structure of the 8-bit blocks. However, it should be approximately valid for the low-frequency content of the jitter. Since it has been shown that low-frequency jitter accumulates much more strongly than high-frequency jitter (see Fig. 3), we are mainly interested in the low-frequency jitter. The agreement of this model with the actual low-frequency jitter will be only approximate because overlap and end effects of the blocks have been neglected.

In the next two sections this model will be applied to special types of patterns to predict the nature of jitter produced by them.

IV. REPETITIVE PATTERN TRANSITIONS

The worst possible jitter occurs when a repetitive pattern which causes an extreme phase lag is suddenly changed to a pattern which causes an extreme phase lead or vice versa. Because this is the worst case of jitter it is worth careful study.

TABLE I — STATIC PHASE SHIFTS OF REPETITIVE 8-BIT PATTERNS

j Pattern Number	Pattern	$\bar{\theta}_j$ Phase Lead Per Repeater (Degrees)	Weight, True Random	Weight, Test Random
1	10000000	−0.7	8	1
2	11000000	+5.9	8	1
3	10100000	+1.3	8	2
4	10010000	−1.8	8	2
5	10001000	−1.8	4	1
6	11100000	+2.0	8	1
7	11010000	+2.2	8	2
8	11001000	−2.4	8	2
9	11000100	−3.1	8	2
10	11000010	−0.2	8	2
11	10101000	+1.8	8	3
12	10100100	−1.3	8	3
13	11110000	+6.8	8	1
14	11101000	+0.7	8	2
15	11100100	−1.8	8	2
16	11100010	+0.9	8	2
17	11011000	+3.1	8	2
18	11010100	−0.4	8	3
19	11010010	−1.5	8	3
20	11001100	+0.9	4	1
21	11001010	−0.9	8	3
22	10101010	0 (reference)	2	1
23	11111000	+2.8	8	1
24	11110100	+1.5	8	2
25	11110010	+1.8	8	2
26	11101100	−1.1	8	2
27	11101010	+2.4	8	3
28	11100110	−0.2	8	2
29	11011010	+0.9	8	3
30	11111100	+5.9	8	1
31	11111010	+3.7	8	2
32	11110110	+3.9	8	2
33	11101110	+2.4	4	1
34	11111110	+5.0	8	1
35	11111111	+11.2	1	0
	10RRRRRR	+0.2 (test random)	sum 255	sum 64

Note: p_j = weight/sum of the weights.

An example of a sudden transition from pattern i to pattern j is shown in Fig. 5. The jitter θ which is injected into each regenerator suddenly jumps from $\bar{\theta}_i$ to $\bar{\theta}_j$. The jitter at the end of a chain of N repeaters can be found by applying (7)

$$\theta_N(t) \approx B \int_{t-(N/B)}^{t} \theta(t)\, dt \tag{14}$$

where

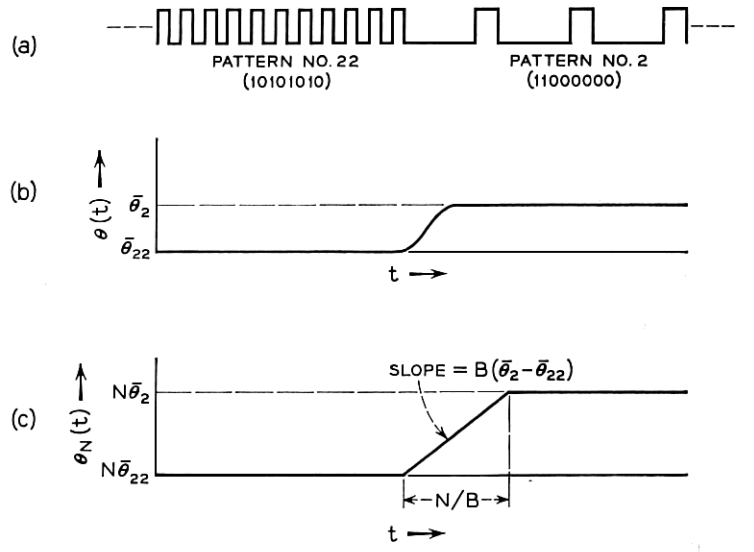

Fig. 5 — Sudden pattern transition: (a) bit pattern, (b) injected jitter, and (c) resultant jitter.

$$\theta(t) = \bar{\theta}_i, \qquad t < 0$$
$$\theta(t) = \bar{\theta}_j, \qquad t > 0.$$

Carrying out the integration, we have

$$\theta_N(t) \approx \begin{cases} N\bar{\theta}_i, & t < 0 \\ N\bar{\theta}_i + B(\bar{\theta}_j - \bar{\theta}_i)t, & 0 < t < \dfrac{N}{B} \\ N\bar{\theta}_j, & t > \dfrac{N}{B}. \end{cases} \tag{15}$$

Equation (15) is plotted in Fig. 5(c).

The approximation used in deriving (15) is valid for low frequencies, and therefore (15) will be a good approximation when N is large.

Note that the total change of phase at the end of N regenerators will be $N(\bar{\theta}_j - \bar{\theta}_i)$. This change is unbounded as the length of the chain increases.

The rate of change of the phase during the transition is

$$\frac{d}{dt}\theta_N(t) = B(\bar{\theta}_j - \bar{\theta}_i). \tag{16}$$

This rate of change of phase, which acts like a frequency change, is limited and independent of N. Further, since $(\bar{\theta}_j - \bar{\theta}_i)$ will be a fraction of a radian, the frequency shift will be well within the bandwidth of the timing filter (B is the half bandwidth). Note that (16) can be derived directly from (3) using the initial-value theorem.

The worst case of jitter, for both phase and frequency deviations, is characterized by the maximum value of $(\bar{\theta}_i - \bar{\theta}_j)$ for all possible pairs of repetitive patterns. This value can therefore be used as a figure of merit for the regenerator. The smaller this figure is, the less will be the maximum phase excursion for a given length of chain, and the less will be the maximum frequency deviation.

It may seem unlikely that such a transition will take place on a real communication channel because simple repetitive patterns are rare. However, they can occur in some systems, particularly when a line is idle. Another example is a PCM system being used to transmit slowly changing analog data.

V. RANDOM PATTERNS

In normal operation a digital channel can be expected to have an essentially random bit pattern. We can find the jitter injected by such a signal by breaking it up into successive 8-bit blocks. The patterns in the blocks are assumed to be independently selected from the set of 8-bit patterns listed in Table I. The patterns do not occur with equal probability. For example, the pattern 10000000 can also occur as 01000000, 00100000, etc., a total of eight distinct forms. However, the pattern 10101010 can occur in only two forms, the other being 01010101. The probability p_j of each pattern is shown in Table I as a relative weight.

From this model of the jitter $\theta(t)$ injected by a random pattern, we can derive the jitter power density Φ. Since the model is valid only for low frequencies, we will ignore the high-frequency structure of Φ.

The spectrum of the model is derived in Appendix B. It is shown that the low-frequency power density is flat (independent of frequency) and that the value of the density is

$$\Phi = 2T_B\sigma^2 \tag{17}$$

where T_B is the time duration of each block.

σ is the standard deviation of the block phase shifts

$$\sigma^2 = \frac{1}{M}\sum_j p_j\left(\bar{\theta}_j - \frac{1}{M}\sum_j p_j\bar{\theta}_j\right)^2 \tag{18}$$

where M is the total number of distinct patterns and p_j is the probability of pattern j.

The value of Φ from (17) can be substituted into (8) to give the jitter at the end of a chain of N repeaters

$$\Phi_N = \left(\frac{B}{\omega}\right)^2 \left| 1 - \left(\frac{1}{1 + j(\omega/B)}\right)^N \right|^2 2T_B\sigma^2. \tag{19}$$

Because Φ is independent of frequency, the plot of jitter in Fig. 3 can also be taken as a plot of the jitter spectrum. The 0 db line represents Φ, the jitter injected in each regenerator.

A number of conclusions can be drawn from the spectra plotted in Fig. 3. The jitter at a given frequency is bounded for all N but the bound grows without limit as the frequency approaches zero. The low-frequency asymptote grows with an amplitude proportional to N.

For very long chains of regenerators, the jitter spectrum approaches

$$\lim_{N\to\infty} \Phi_N \to \left(\frac{B}{\omega}\right)^2 \Phi. \tag{20}$$

The mean-square jitter can be found by integrating the jitter spectrum over all frequencies (see Appendix C). The result is

$$\overline{\theta_N^2} = \Phi B P(N) \tag{21}$$

where

$$\Phi = 2T_B\sigma^2$$

B is the half bandwidth of the timing tank, and
P_N is given in Table II for values of N from 1 to 100.

For chains of more than 100 repeaters,

$$\overline{\theta_N^2} \approx \tfrac{1}{2}\Phi BN. \tag{22}$$

Therefore, we see that the mean square jitter in long chain increases as N and the root mean square jitter increases as the square root of N. Rowe[4] and DeLange[2] have shown that root mean square jitter due to nonsystematic sources increases only as the fourth root of N. Therefore, systematic jitter must dominate in sufficiently long chains.

It is interesting that the total rms jitter is unbounded, even though the jitter components near any one frequency are bounded. This behavior has been confirmed by Kinariwala[6] for a very general model of a regenerator. The explanation of the paradox lies in the fact that the bound for the very low-frequency components becomes very large as the chain grows longer.

TABLE II — $\overline{\theta_N^2} = \Phi BP(N)$

N	$P(N)$
1	0.250
2	0.625
3	1.031
4	1.453
5	1.887
6	2.308
7	2.753
8	3.200
9	3.652
10	4.105
20	8.74
30	13.27
40	18.22
50	23.01
60	27.82
70	32.64
80	37.48
90	42.32
100	47.18

For $N > 100$, $P(N) \approx N/2$.

Another interesting property of (21) is that the jitter power is proportional to the timing filter bandwidth. This confirms the intuitively obvious fact that high-Q tank circuits in the regenerators will reduce jitter.

The amplitude distribution of jitter is also interesting. In principle, it is truncated, since the amplitude is limited by the worst case bounds discussed in the previous section. However, the general shape of the distribution will be shown to be Gaussian, and for long chains of repeaters the truncation occurs far out on the tail of the distribution.

To study the amplitude distribution, we will use (7)

$$\theta_N(t) \approx B \int_{t-(N/B)}^{t} \theta(t)\, dt. \tag{23}$$

The approximation is valid for low frequency and therefore is good for long chains, where low frequencies dominate. When we consider $\theta(t)$ to be a sequence of rectangular blocks of duration T_B we can write

$$\theta_N(pT_B) \approx BT_B \sum_{p-M}^{p} \theta_i\,. \tag{24}$$

Where $\theta_N(pT_B)$ is the jitter at time pT_B

$$M \approx \frac{N}{T_B B} \approx \frac{QN}{\pi K} \text{ (nearest integer)}.$$

K is the number of bits in each block of duration T_B.

Equation (24) shows that the jitter can be expressed as the sum of M independent samples from the set of block patterns. It is well known (central limit theorem) that such a sum has an amplitude distribution which approaches a Gaussian form as M becomes large.

To see how well a distribution of this nature approaches the Gaussian shape, a sample problem was computed. The probability distribution of θ_j was assumed to consist of five equally spaced impulses of equal probability. Actually, the distribution would probably be better spread than this. The value of M was taken as 50. This corresponds to a chain of 13 repeaters with a Q of 100 and the block length taken as 8 bits.

The cumulative probability deviation for this case is plotted on probability paper in Fig. 6. The straight line represents a true Gaussian distribution. Since the distribution is symmetrical, only half of it has been plotted. A normalized deviation of 1 corresponds to the standard deviation. Truncation of the example shown in Fig. 6 occurs at a normalized deviation of 10.

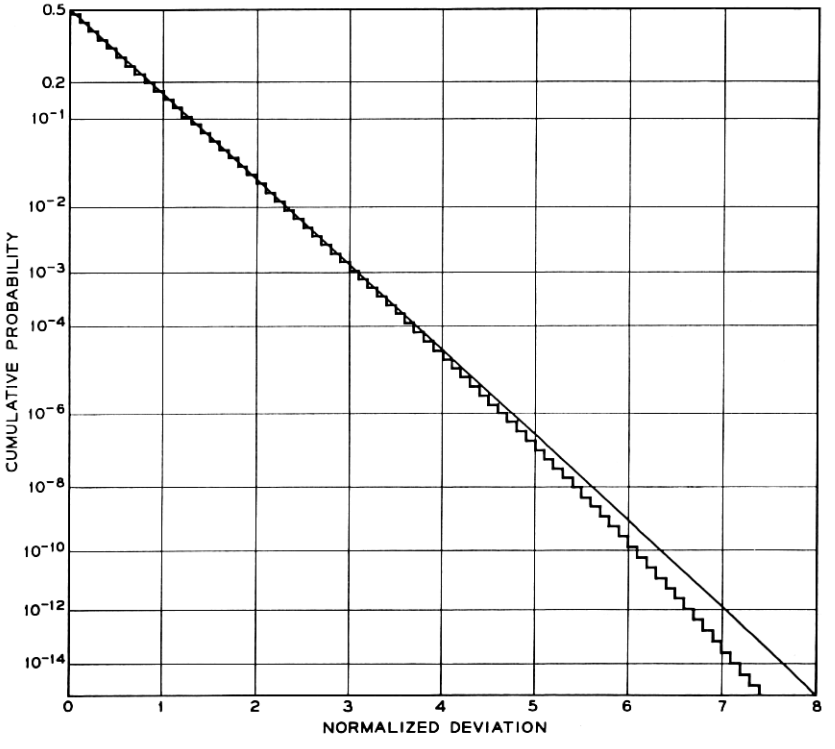

Fig. 6 — Amplitude distribution of jitter, true Gaussian and computed.

Fig. 6 shows that the distribution is Gaussian down to a cumulative probability of one part in 10^{10}. This seems to be sufficient justification for assuming a Gaussian distribution for long chains of regenerators.

In summary, a random pattern introduces jitter with a flat spectrum into each regenerator. The power density of this jitter can be predicted from measurements with a set of repetitive test signals.

The jitter at the end of a long chain of N repeaters is approximately Gaussian distributed, with an rms value which increases as the square root of N, without bound. The power density approaches a bound which is inversely proportional to the square of frequency.

VI. EXPERIMENTS

Measurements were made both in the laboratory and in a field installation which are in agreement with the theory mentioned in the previous sections.

In the laboratory, trains of one to ten repeaters were used, while trains of 14 to 84 repeaters were available at a field site located between Passaic and Newark, New Jersey. The laboratory repeaters were bipolar regenerators using ideal forward acting self-timing.[7] The field repeaters were quite similar to these generally, but differed in their physical shape, and in a minor respect in their clock circuitry. The interrepeater spacings were controllable in the laboratory only. In the field, all equipment was installed in one central office, the signals being sent on repeatered lines to other offices and then returned on separate lines. The field situation was such that crosstalk and other interference was negligible. Since lines could not be terminated in the field conveniently at places other than central offices, the minimum number of repeaters that could be used was 14. All the different line lengths tested in the field were thus multiples of 14.

The repeatered lines were driven by a word generator which could emit a train of bipolar pulses, and the necessary clock references for the phase measuring equipment. The generator could emit any of the fixed patterns possible with 8 digits, or a random pattern, or a combination of fixed and random. In addition, it could switch between two different fixed patterns at rates of several kc or less. A restriction on the patterns in this case was that all the pulses in the less dense pattern must also be present in the denser one.

The phase detector used for measuring the jitter operated in the following manner. The reference clock from the word generator was used to set a flip-flop which was reset by a clock derived from the last repeater in the train. Jitter in this clock would cause the flip-flop to gener-

ate a duration-modulated pulse. To extend the measuring range, both clocks were divided by two before being sent to the flip-flop. This operation did not reduce the amount of jitter presented to the instrument, however. The jitter information contained in the duration variations of the flip-flop output pulses was converted to corresponding amplitude variations by passing those pulses through suitable low-pass filters and amplifiers. This, of course, is a standard way of demodulating duration-modulated pulses.

The jitter information, now in the form of voltage variations, was passed to a detector. For measuring fixed pattern shifts, an oscilloscope and camera were used. For random patterns, a true rms voltmeter and high-quality tape recorder served as detectors.

A typical photograph of transitions between two fixed patterns is shown in Fig. 7. Note the close resemblance to the waveform derived from the model (Fig. 5c). It was shown in Section IV that the total change of phase at the end of N regenerators should be N times the phase difference between the two fixed patterns in question for one regenerator. Fig. 8 shows the total change of phase plotted against N for transitions between various fixed patterns. The relations are clearly linear. It is also apparent that pattern density is not the only factor influencing phase shift, as was mentioned in Section III. Note for example the transitions from 10000000 to 11000000 (1/8 to 2/8) and 10000000 to 10001000 (1/8 to 1/4). Both have equal density change but phase changes of different sign and amplitude. Examination of Fig. 8 would lead one to believe that the effect of intersymbol interference on phase

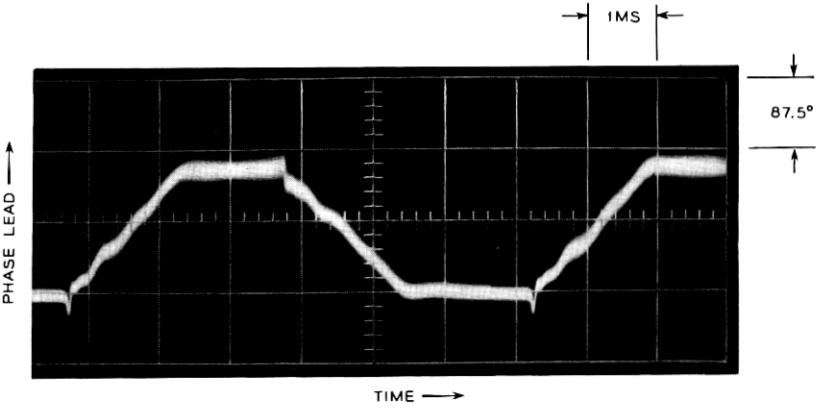

Fig. 7 — Photograph of phase shift due to a transition from a 1/8 pattern (top) to an 8/8 pattern (bottom), with 84 repeaters; phase scale, 87.5 degrees/cm; time scale, 1 msec/cm.

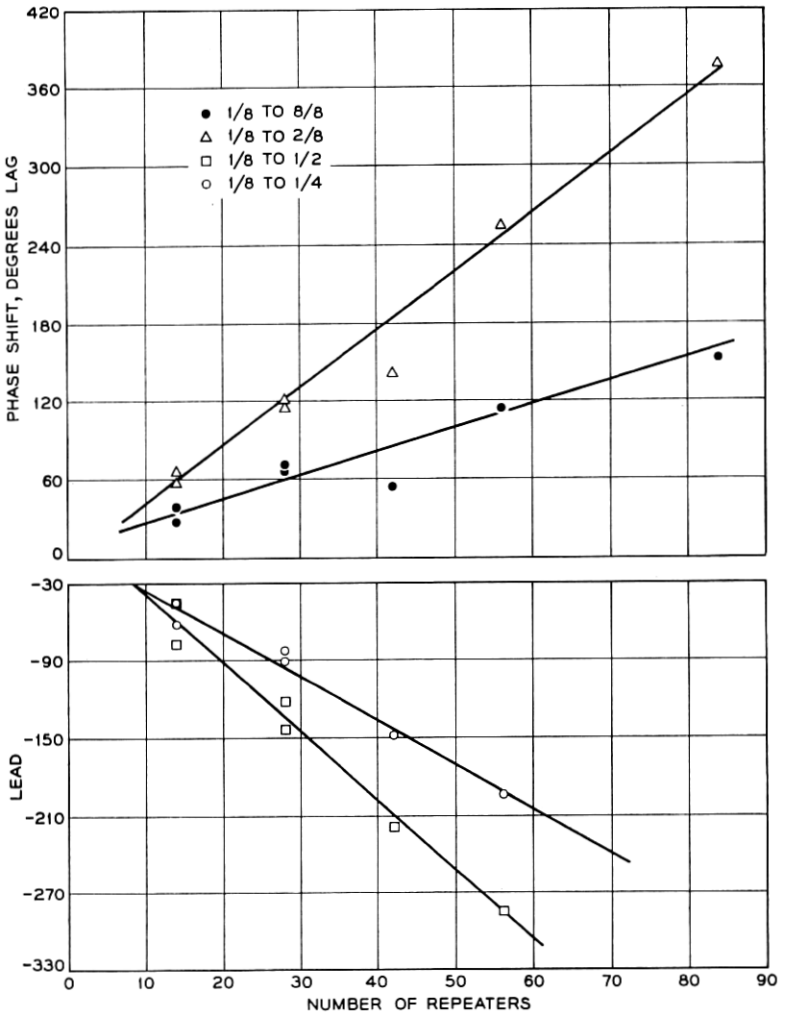

Fig. 8 — Steady-state phase shift between fixed patterns.

shift is comparable to the effect of density. The transitions from 1/8 to 1/4 and 1/8 to 1/2 (10101010) involve patterns with little or no intersymbol interference. A doubling of density between 1/4 to 1/2 causes about a 50 per cent increase in phase shift. Changing the pattern geometry to 2/8, which has intersymbol interference, is sufficient to cause a change in the algebraic sign of the phase shift. In the case of the 1/8 to 8/8 (all pulse) transition, the effects of density and intersymbol inter-

ference partially cancel each other, but the resultant shift indicates that the intersymbol interference is the larger.

Equation (16) states that the rate of change of phase during the transition between two given fixed patterns is proportional to the half bandwidth of the timing filter and to the phase change between the two patterns. Restating this equation

$$\frac{d}{dt}\theta_N(t) = B(\bar{\theta}_j - \bar{\theta}_i) = \frac{\pi f_o}{Q}\Delta\theta \tag{25}$$

where $\Delta\theta$ is the phase change per repeater between the two patterns, f_o is the pulse repetition frequency (timing filter center frequency), and Q is the quality factor of the tank. Fig. 9 shows the measured rate of change of phase in degrees per millisecond plotted against the absolute value of the phase change per repeater. The slopes were obtained from photographs of the transients during the various transitions. Using the known pulse repetition frequency, (25), and the best line fit from Fig. 9, it is possible to arrive at a value of Q for the average repeater tank. This is found to be 72. This figure is quite compatible with the expected values of loaded Q for repeater timing tanks (about 80).

To check the effect of repeater spacing, the phase shift for one pattern transition (1/8 to 8/8) was measured in the laboratory with the repeaters first correctly spaced at 6000-foot intervals, and then spaced at 5000-foot intervals with no compensation. This is a more severe condition than would be encountered in actual repeater practice. The data of Fig. 10 show that shortening the span has little effect on phase shift. Photographs showed the transient behavior to be unaffected also.

The properties of jitter caused by a random pattern were investigated with a special quasi-random signal. The pattern was constrained to have one forced pulse followed by one forced space at the beginning of every block of eight slots, the remaining six spaces being filled with random pulses. Forcing the pulse was necessary to ensure that the clock of the self-timed repeaters did not die out. There is no particular reason for forcing the space except that it kept the over-all pulse density at one half.

In testing the field repeatered lines with this quasi-random pattern, the output from the phase detector was recorded on tape and studied later with amplitude and frequency distribution analyzers and a true rms voltmeter. The results of these measurements are plotted in Figs. 11–15, and will be used to corroborate the theoretical predictions of Section V.

The measured spectral distributions of the output data are shown in

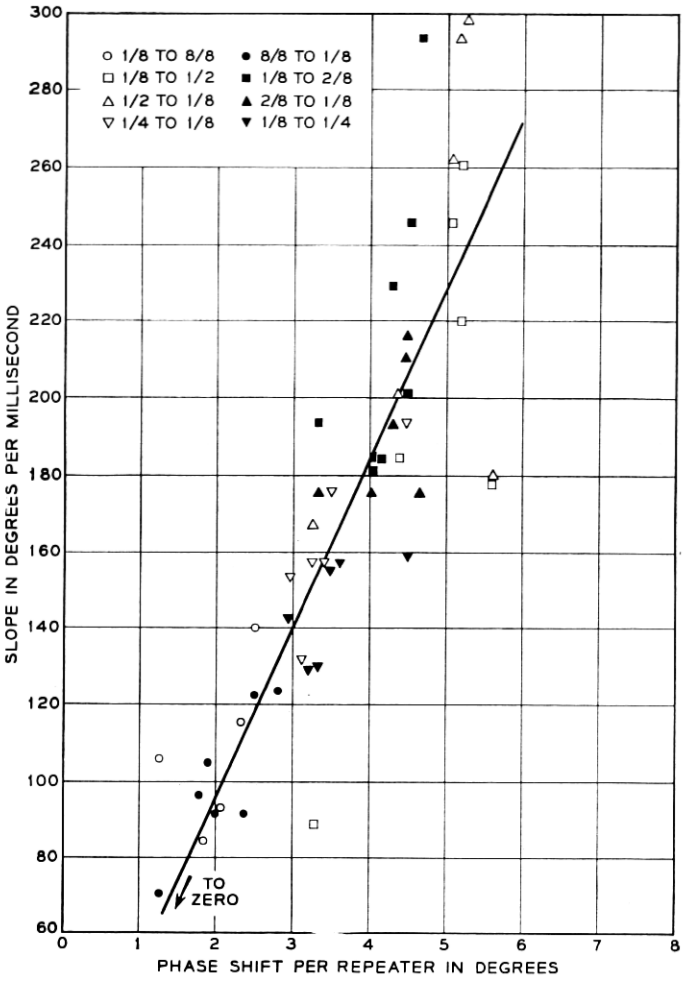

Fig. 9 — Measured rate of change of phase versus the absolute value of the phase change per repeater.

Fig. 11. We have shown in Section V that the spectrum of random jitter injected at each repeater is flat; therefore, the spectrum at the end of a chain of repeaters should have the shape of the corresponding jitter transfer function, plotted in Fig. 3. A comparison of Figs. 3 and 11 shows that they are in excellent agreement, even to the details of the nulls. A direct comparison of the measured and theoretical spectra for a chain of 84 repeaters is shown in Fig. 12. The theoretical curve is given by (8).

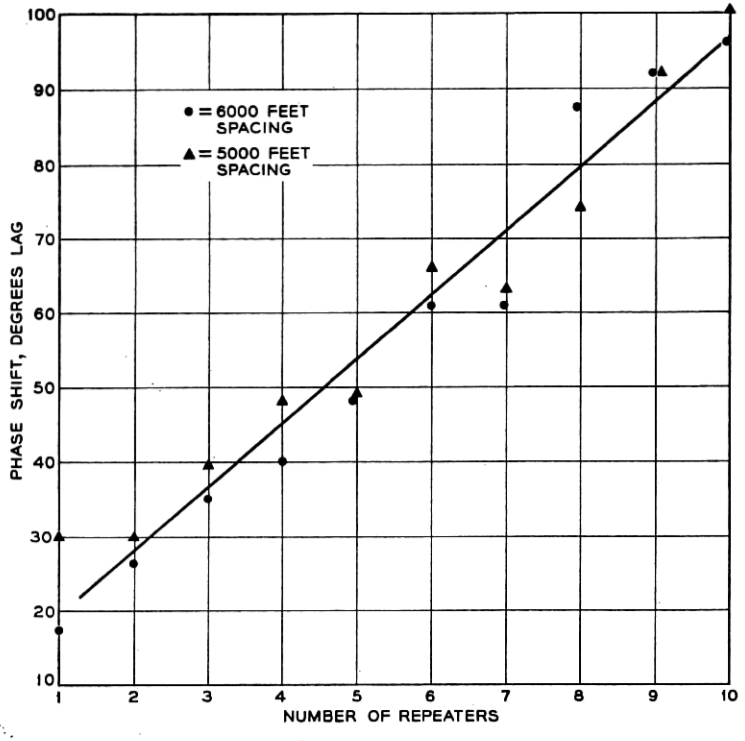

Fig. 10 — Measurement of the effect of repeater spacing.

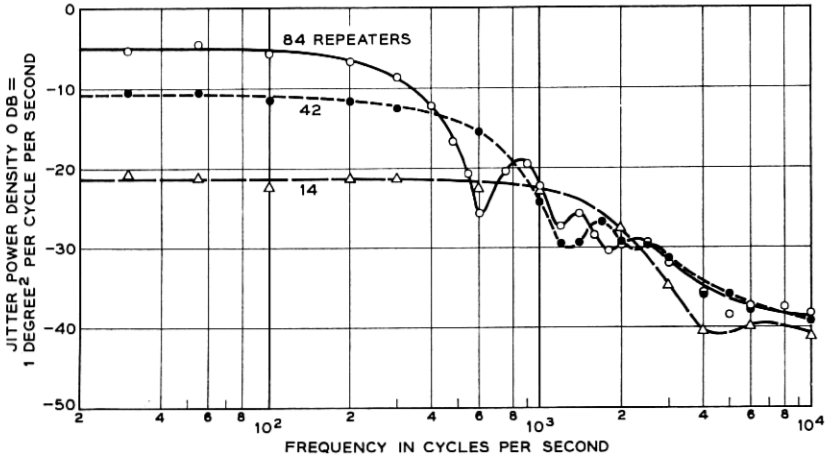

Fig. 11 — Measured spectral distributions for a random pattern (10- - - - - -).

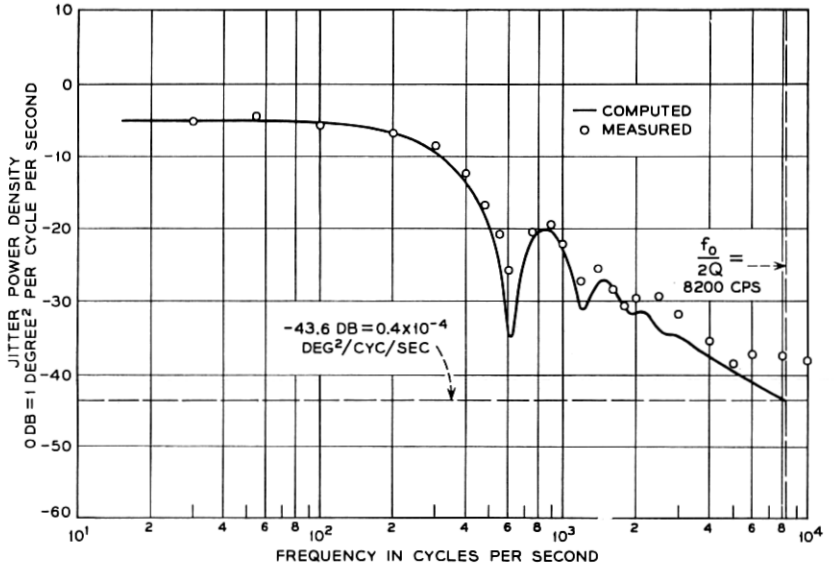

Fig. 12 — Comparison of measured and theoretical spectra for a chain of 84 repeaters.

The two parameters Φ and B were adjusted to give the best fit. The corresponding jitter injection density was 0.44×10^{-4} degrees squared per cycle per second and the tank Q was 94 (compare a value of 72 from pattern transition slopes).

Inspection of (8) shows that the jitter amplitude density at very low frequencies should be directly proportional to the number of repeaters. This is a consequence of assuming systematic jitter sources. The measured low-frequency jitter density is plotted against the number of repeaters in Fig. 13. The curve is indeed linear. The slope of this line can be used to find the power density of jitter injected at each repeater (0.44×10^{-4} degrees squared per cycle per second). The rms value of the jitter was measured for each chain of repeaters. The result is shown in Fig. 14. The solid curve is plotted from (21), with the product (ΦB) adjusted for a best fit. Using a value of 0.44×10^{-4} for Φ (from Fig. 13) the value of Q is found to be 69, in good agreement with the value 72 found from slope data. The dotted line in Fig. 14 is the asymptote for long chains, given by (22).

The amplitude distribution of the random jitter was also measured. All of the curves were Gaussian in form, with no indication of truncation within the limits of the amplitude analyzer. A typical distribution (54

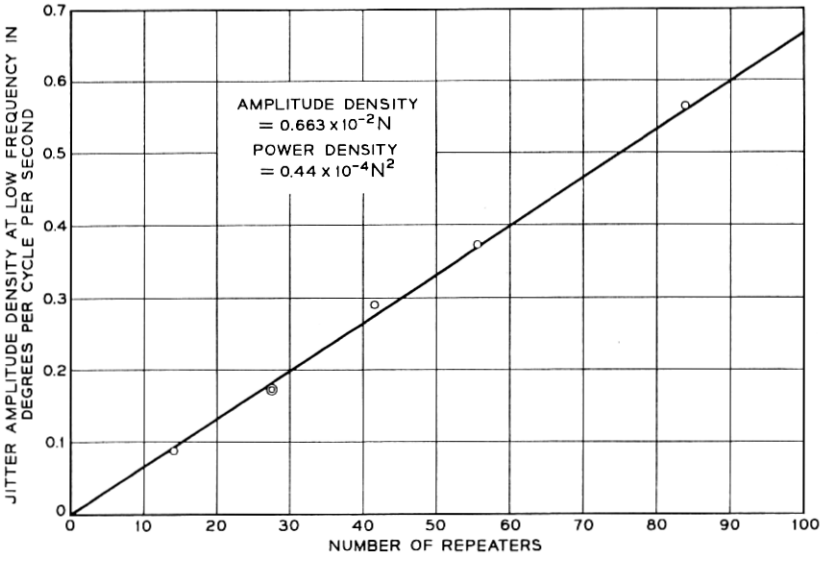

Fig. 13 — Measured low-frequency jitter amplitude density versus the number of repeaters in the chain.

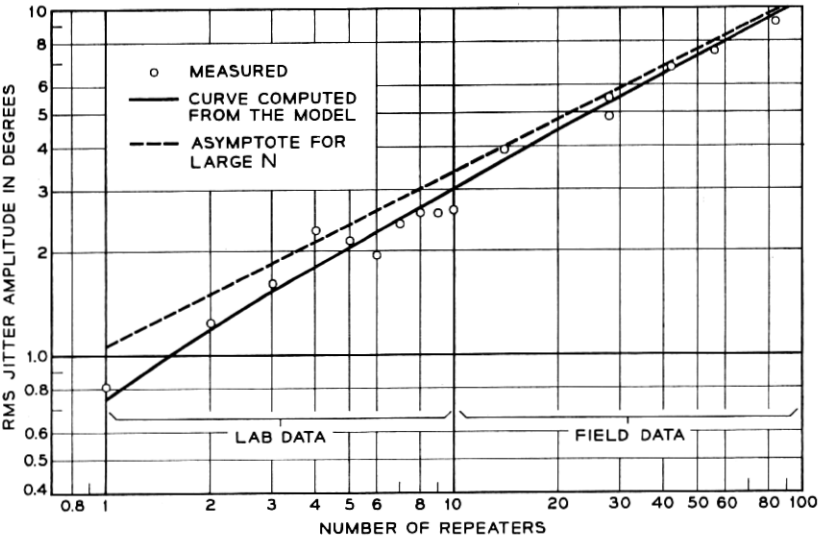

Fig. 14 — Root-mean-square jitter due to a random pattern (10------) versus the number of repeaters in the chain, measured and calculated.

repeaters) is plotted on probability paper in Fig. 15. Note that the curve extends to amplitudes which have a probability of only 2×10^{-4} of being exceeded, with no sign of truncation.

The data described above establish all the predicted properties of the model. However, the important parameter Φ, the jitter power density injected at each regenerator, has been measured using random patterns on long chains of repeaters. Equation (17) relates Φ to measurements with simple repetitive patterns on a few repeaters. This allows the performance of long chains of repeaters to be predicted from short chains, measured in the lab. To test the method, a chain of 10 repeaters was set up in the lab, as described above. The average phase shift of these repeaters was measured for every possible 8-bit repetitive pattern, as shown in Table I. Pattern 22 was used as a reference.

The standard deviation of the phase shifts was found to be 2.225°, calculated according to (18). The weights used were those for the test random pattern. Using this value, (17) was used to find the power density Φ, yielding a value of 0.513×10^{-4} deg²/cps. Since the measured

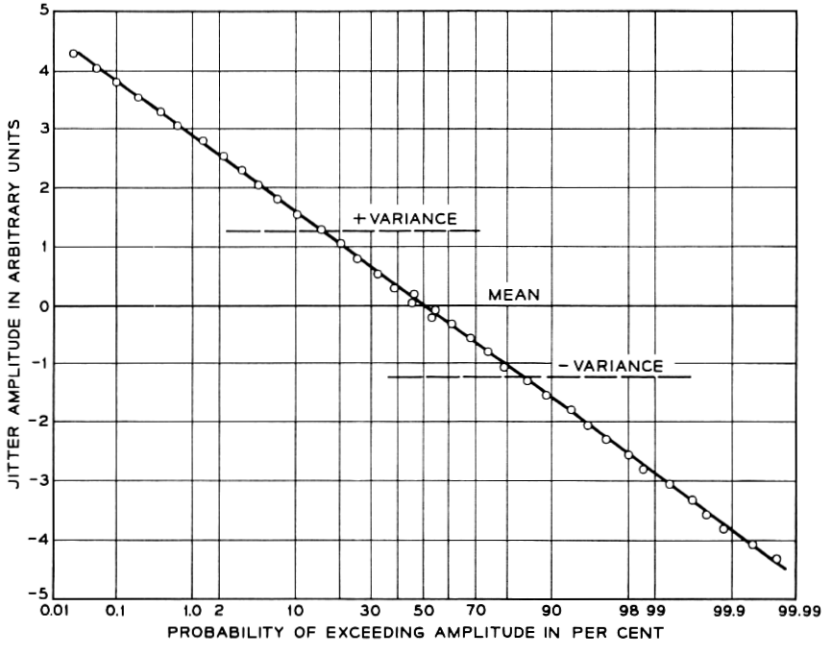

Fig. 15 — Typical amplitude distribution of jitter due to a random pattern (10- - - - - -) (54 repeaters).

value on long chains in the field was 0.44×10^{-4} deg²/cps, this result validates the assumptions made in deriving the model and shows that simple measurements in the lab can adequately predict the behavior of long chains in the field.

VII. ALIGNMENT JITTER

We have shown that jitter is unbounded; however, we will now show that the nature of jitter is such that it will not contribute strongly to digital errors in the regenerator chain.

Alignment jitter has been defined by Rowe[4] as deviations in alignment between the input signal pulse and the corresponding timing pulse. In terms of our model, the output jitter of one repeater is the input jitter for the next, and the timing jitter of a repeater becomes its output jitter. Therefore, we will redefine alignment jitter in a particular repeater as the difference between its output jitter and the output jitter of the preceding regenerator:

$$\theta_{aN} = \theta_N - \theta_{N-1} \tag{26}$$

Substituting from (3)

$$\Theta_{aN}(s) = \Theta(s) \left(\frac{1}{1 + (s/B)}\right)^N \tag{27}$$

Since the jitter injected at each repeater is bounded, we can show by a straightforward analysis that the alignment jitter is bounded, and further, the bound does not increase as the length of the chain of repeaters increases. (See Appendix D.) These properties are easily seen if we consider simple pattern transition. In that case the alignment jitter increases from zero to a value equal to the phase shift due to the final pattern. (See Fig. 16.) An important assumption in our discussion of

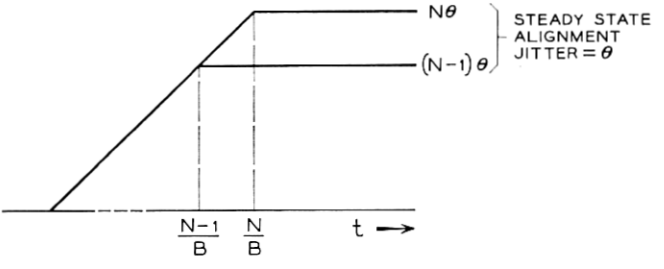

Fig. 16 — Alignment jitter for a fixed pattern.

alignment jitter is that the frequencies and Q's of the timing filters are identical.

The error margin for random noise interference has been measured at the first and last repeater in a long chain of repeaters in the field. No significant difference was found. In addition, analog measurements on voice channels in T1 carrier terminals showed no noticeable change as the length of the repeatered line coupling these terminals was increased from about 11 to about 130 miles (14 repeaters to 154 repeaters).

It is clear that even though jitter becomes quite large in long chains, the error margin of the repeaters does not decrease.

VIII. SUMMARY

We have measured the jitter in a field installation of the T1 24-channel PCM carrier system. The maximum number of repeaters in tandem was 84. The jitter was produced by pattern variations in the signal.

The largest jitter observed is produced by a sudden transition from one repetitive pattern to another. This causes a steady-state phase shift which increases linearly with the number of repeaters. The amount of the shift depends on the patterns used and is of the order of two degrees per repeater. The rate of change of the phase shift also depends on the patterns used and is of the order of 2000 radians per second. This phase shift slope becomes independent of the number of repeaters. These measurements are consistent with the work of R. C. Chapman.

Jitter produced by random signals has the character of noise. The root mean square phase deviation after 84 repeaters is about 10°. For long chains of repeaters the rms jitter increases in proportion to the square root of the number of repeaters. At a given frequency, the jitter power density approaches a limit as the number of repeaters grows large. However, at low frequencies this limit is very large and is not approached for a reasonable number of repeaters. This low-frequency jitter power density is directly proportional to the number of repeaters. Therefore, for long chains of repeaters, the jitter is concentrated at low frequencies. For 84 repeaters the jitter power is mostly below 400 cycles per second. It is interesting to note that this is much less than the half bandwidth of the timing filters, which is about 10,000 cycles per second. The amplitude distribution of jitter is Gaussian.

We have derived a model which is in agreement with our measurements. This model assumes that the causes of jitter are systematic: that is, the same at each repeater. While nonsystematic effects are undoubtedly present, their jitter does not accumulate as rapidly as that

due to systematic sources and is not significant in long chains. We further assume that only the low-frequency components of jitter are important, since high-frequency components are strongly attenuated by the timing filters. The model quantitatively predicts the measurements of random jitter from measurements of the steady-state phase shift of 8-bit repetitive patterns.

We have shown that the model is valid for many sources of jitter, including amplitude-to-phase conversion, intersymbol interference, and finite width effects. It is also valid for the effects of mistuning in very long chains of repeaters, although mistuning was not an important source of jitter in the repeaters we measured.

IX. ACKNOWLEDGMENTS

This work was made possible by the availability of the field installation of the T1 system. We are grateful to Mr. F. K. Harvey for the loan of the tape recording equipment used in gathering field measurements and to Mr. M. R. Aaron for his timely suggestions and criticisms during the writing of this paper. Essential parts of the theoretical work were done by Messrs. S. O. Rice, W. R. Bennett, and A. J. Goldstein.

APPENDIX A

Amplitude and Jitter Transfer Functions of a Single-Tuned Tank Circuit

The following argument is based on work by S. O. Rice on the analysis of FM systems. The timing wave is extracted from the signal by a high-Q single-tuned filter. Therefore, for the input to this filter, we need only consider that component of the signal which is near the bit rate. This component is amplitude modulated by the pulse density and phase modulated by the jitter.

Therefore, let the signal incident on the filter be given by the real part of

$$v_i(t) = \exp [j\omega_c t + j\theta(t) + a(t)] \tag{28}$$

where ω_c is the bit frequency, and $\theta(t)$ and $a(t)$ are arbitrary functions of time with the restriction that their time derivatives are small.

We will write the output of the filter as

$$v_o(t) = \exp [j\omega_c t + j\theta_o(t) + a_o(t)]. \tag{29}$$

Further, if we express the impulse response of the filter as

$$g(t) = \int_{-\infty}^{\infty} Y(j\omega) e^{j\omega t}\, df \tag{30}$$

we have

$$v_o(t) = \int_{-\infty}^{\infty} \exp\left[j\omega_c(t-x) + j\theta(t-x) + a(t-x)\right] g(x)\,dx. \quad (31)$$

Equating (29) and (31), we have

$$j\theta_o(t) + a_o(t) = \ln \int_{-\infty}^{\infty} \exp\left[j\theta(t-x) + a(t-x) - j\omega_c x\right] g(x)\,dx. \quad (32)$$

We will assume that the transfer function of the filter is zero for frequencies above $(f_c + r)$ and below $(f_c - r)$, for some r. When we impose this condition on (30) and make the change of variable

$$f = f_c + f' \quad (33)$$

we have, to a high degree of approximation

$$j\theta_o(t) + a_o(t) = \ln \int_{-\infty}^{\infty} \exp\left[j\theta(t-x) + a(t-x)\right] h(x)\,dx \quad (34)$$

where

$$h(x) = \frac{1}{2\pi} \int_{-r}^{r} Y(j\omega_c + j\omega')\, e^{j\omega' x}\, d\omega'. \quad (35)$$

For a tuned tank

$$Y(j\omega_c + j\omega) \approx \frac{1}{1 + j(\omega/B)} \quad (36)$$

where B is the half bandwidth.

For a high-Q filter we may let r in (35) go to infinity, whereupon

$$h(x) = \begin{cases} 0, & x < 0 \\ Be^{-Bx}, & x > 0. \end{cases} \quad (37)$$

Now we return to the evaluation of (34), which is our problem. We will approximate

$$e^{j\theta(t-x)+a(t-x)} = e^{a(t)+j\theta(t)} \sum_{0}^{\infty} \frac{(-x)^n}{n!} F_n(t) \quad (38)$$

where

$$F_n(t) = e^{-j\theta(t)-a(t)} \frac{d^n}{dt^n} e^{a(t)+j\theta(t)}. \quad (39)$$

We now define

$$m_n = \int_{-\infty}^{\infty} x^n h(x)\, dx \tag{40}$$

or

$$m_n = n!B^{-n}. \tag{41}$$

Then from (38) and (40) we have

$$\int_{-\infty}^{\infty} \exp\,[j\theta(t-x) + a(t-x)]h(x)\, dx = e^{j\theta(t)+a(t)}\left\{1 + \sum_{n=1}^{\infty} \frac{(-1)^n m_n}{n!} F_n(t)\right\}. \tag{42}$$

Now in general

$$\ln\left(1 + \sum_{1}^{n} \frac{\alpha_n t^n}{n!}\right) = \frac{t}{1!}\alpha_1 + \frac{t^2}{2!}(\alpha_2 - \alpha_1^2) + \frac{t^3}{3!}(\alpha_3 - 3\alpha_2\alpha_1 + 2\alpha_1^3) + \cdots. \tag{43}$$

So if we take $t = -1$, $\alpha_n = m_n F_n(t)$, we have

$$\begin{aligned}\ln \int_{-\infty}^{\infty} \exp\,[j\theta(t-x) + a(t-x)]h(x)\, dx &= j\theta_o(t) + a_o(t) \\ &= a(t) + j\theta(t) + \left[-\frac{m_1F_1}{1!} + \frac{1}{2!}(m_2F_2 - m_1^2F_1^2)\right. \\ &\quad \left. - \frac{1}{3!}(m_3F_3 - 3m_2m_1F_2F_1 + 2m_1^3F_1^3) + -\cdots\right].\end{aligned} \tag{44}$$

Now we replace the F_n by their values from (39), and after some manipulation we have

$$a_o(t) + j\theta_o(t) = \int_{-\infty}^{\infty} [j\theta(t-x) + a(t-x)]h(x)\, dx \tag{45}$$

+ (terms in powers of the derivatives of $\theta(t)$ and $a(t)$ normalized to the half bandwidth)

+ (cross products of the derivatives of $\theta(t)$ and $a(t)$ normalized to the half bandwidth)

where we have made use of the fact that

$$[a(t) + j\theta(t)] - m_1[a'(t) + j\theta'(t)] + \frac{m_2}{2}[a''(t) + j\theta''(t)] + \cdots = \int_{-\infty}^{\infty} [a(t - x) + j\theta(t - x)]h(x)\,dx. \tag{46}$$

Now, if we neglect powers and cross products of all the derivatives of $\theta(t)$ and $a(t)$, and use the value of $h(x)$ from (37), we have

$$a_o(t) + j\theta_o(t) = \int_0^t Be^{-Bx}a(t - x) + j\theta(t - x)\,dx. \tag{47}$$

Equating real and imaginary parts and recognizing the convolution integral, we have

$$\Theta_o(s) = \frac{1}{1 + (s/B)}\,\Theta(s) \tag{48}$$

and

$$A_o(s) = \frac{1}{1 + (s/B)}\,A(s). \tag{49}$$

The relationship given in (48) is one of the results we are seeking. The amplitude modulating signal, however, is $e^{a(t)}$, not $a(t)$. If now we restrict $a(t)$ to be small, then

$$e^{a(t)} \approx 1 + a(t).$$

From (47) it is clear that if $a(t)$ is small, then $a_o(t)$ is small, and then the output amplitude modulation

$$e^{a_o(t)} \approx 1 + a_o(t).$$

Then we see that (49) gives the relationship in the transform domain between the varying term of the input AM and the varying term of the output AM.

APPENDIX B

Power Density of a Jitter Produced by a Random Pattern

The jitter $\theta(t)$ produced by a series of 8-bit blocks may be represented by

$$\theta(t) = \sum_{-\infty}^{\infty} \bar{\theta}_n A(t - n8T_o) \tag{50}$$

where

T_o is the bit interval,

$\bar{\theta}_n$ is the phase shift that would be produced by the pattern of block n, in a repetitive pattern, and

$$A(t) = \begin{cases} 1, & -4T_o < t < 4T_o \\ 0, & |t| > 4T_o . \end{cases}$$

The patterns in successive blocks are statistically independent, and $\bar{\theta}_n$ can be taken to have zero mean. When we add an arbitrary starting time we make the process whose sample functions are given by (50) stationary. Then the autocorrelation function can be shown to be

$$\psi(\tau) = \sigma^2 \Delta(\tau) \tag{51}$$

where

$$\Delta(\tau) = \begin{cases} \left(1 + \dfrac{\tau}{8T_o}\right), & -8T_o < \tau < 0 \\ \left(1 - \dfrac{\tau}{8T_o}\right), & 0 \leqq \tau < 8T_o \\ 0, & |\tau| \geqq 8T_o \end{cases}$$

where τ is the time difference, and σ is the standard deviation of $\bar{\theta}_n$.

The one-sided power density is given by

$$\Phi(\omega) = 2 \int_{-\infty}^{\infty} \psi(\tau) e^{-j\omega\tau} \, d\tau. \tag{52}$$

Substituting (51) in (52) gives

$$\Phi(\omega) = \frac{4\sigma^2}{\omega} \frac{\sin^2 \omega 4T_o}{\omega 4T_o}. \tag{53}$$

Applying L'Hospital's rule we obtain

$$\Phi(0) = 2(8T_o)\sigma^2. \tag{54}$$

Furthermore, it is clear from (53) that at zero frequency the slope of the power density is zero, and because T_o is small for the system under consideration we may assume to a very high degree of accuracy that over the band of frequencies which are of interest, the power density is flat.

The values of $\bar{\theta}_n$ have a discrete probability distribution, indicated in Table I. Therefore,

$$\sigma^2 = \frac{1}{M} \sum_j p_j \left(\bar{\theta}_j - \frac{1}{M} \sum_j p_j \bar{\theta}_j\right)^2 \tag{55}$$

where p_j is found by dividing the weights by the sum of the weights. M is the total number of distinct patterns.

APPENDIX C

Integration of the Jitter Spectrum

We are indebted to A. J. Goldstein for the following integration.

The spectrum of jitter at the end of a chain of N repeaters was given in the section on the model in (8).

$$\Phi_N(\omega) = \Phi \frac{B^2}{\omega^2}\left[1 - \left(\frac{1}{1+j(\omega/B)}\right)^N\right]^2. \tag{56}$$

The mean-square jitter is given by

$$\begin{aligned}\overline{\theta_N^2} &= \frac{1}{2\pi}\int_0^\infty \Phi_N(\omega)\, d\omega \\ &= \frac{\Phi}{2\pi}\int_0^\infty \frac{B^2}{\omega^2}\left|1 - \left(\frac{1}{1+j(\omega/B)}\right)^N\right|^2 d\omega \qquad (57)\\ &= \frac{\Phi B}{2\pi}\int_0^\infty \frac{1}{\omega^2}\left|1 - \left(\frac{1}{1+j\omega}\right)^N\right|^2 d\omega \\ \overline{\theta_N^2} &= \Phi B P(N) \qquad (58)\end{aligned}$$

where

$$\begin{aligned}P(N) &= \frac{1}{2\pi}\int_0^\infty \frac{1}{\omega^2}\left|1 - \left(\frac{1}{1+j\omega}\right)^N\right|^2 d\omega \\ P(N) &= \frac{1}{2\pi}\int_0^\infty \frac{1}{\omega^2}\left[1 - \left(\frac{1}{1+j\omega}\right)^N\right]\left[1 - \left(\frac{1}{1-j\omega}\right)^N\right] d\omega \\ &= \frac{1}{2\pi}\int_0^\infty \frac{1}{\omega^2}\left[1 - \left(\frac{1}{1+j\omega}\right)^N - \left(\frac{1}{1-j\omega}\right)^N\right. \\ &\qquad \left. + \left(\frac{1}{1+\omega^2}\right)^N\right] d\omega. \end{aligned} \tag{59}$$

Let us introduce the dummy variable a and define

$$\begin{aligned}\Sigma(a) &= \sum_{N=0}^{\infty} P(N) a^N \\ &= \frac{1}{2\pi}\int_0^\infty \frac{1}{\omega^2}\sum_{N=0}^{\infty}\left[a^N - \left(\frac{a}{1+j\omega}\right)^N - \left(\frac{a}{1-j\omega}\right)^N\right. \\ &\qquad \left. + \left(\frac{a}{1+\omega^2}\right)^N\right] d\omega. \end{aligned} \tag{60}$$

We recognize that each of the terms in the summation of (60) is a geometric series whose sum is given by

$$\sum_0^\infty r^n = \frac{1}{1-r}. \tag{61}$$

Using this, we can write

$$\begin{aligned}\Sigma(a) &= \frac{1}{2\pi}\int_0^\infty \frac{1}{\omega^2}\left[\frac{1}{1-a} - \frac{1}{1-\dfrac{a}{1+j\omega}} - \frac{1}{1-\dfrac{a}{1-j\omega}} + \frac{1}{1-\dfrac{a}{1+\omega^2}}\right]d\omega \\ &= \frac{1}{2\pi}\int_0^\infty \left[\frac{a}{1-a}\frac{1}{\omega^2} - \frac{2a(1-a)}{\omega^2[\omega^2+(1-a)^2]} + \frac{a}{\omega^2[\omega^2+(1-a)]}\right]d\omega.\end{aligned} \tag{62}$$

All of the terms above can be integrated by using standard tables. The result is

$$\Sigma(a) = \sum_{N=0}^\infty P(N)a^N = \frac{1}{2}\left[\frac{a}{(1-a)^2} - \frac{1}{2}\frac{a}{(1-a)^{3/2}}\right]. \tag{63}$$

If we expand the right-hand term of (63) in a power series, the coefficients of the a^N will be the $P(N)$

$$P(N) = \frac{1}{2}\left[N - \frac{1}{2}\frac{(2N-1)!}{4^{(N-1)}[(N-1)!]^2}\right]. \tag{64}$$

For values of N greater than 5 we can approximate the factorials by Stirling's formula

$$n! \approx \sqrt{2n\pi}\,(n/e)^n. \tag{65}$$

The result is

$$P(N) \approx \frac{1}{2}\left(N - \frac{1}{\sqrt{\pi}}\frac{N-\frac{1}{2}}{\sqrt{N-1}}\right). \tag{66}$$

For $N > 10$ we can make the further approximation

$$P(N) \approx \frac{1}{2}\left(N - \frac{1}{\sqrt{\pi}}\sqrt{N}\right). \tag{67}$$

And for $N > 100$

$$P(N) \approx N/2. \tag{68}$$

Values of $P(N)$ from 1 to 100 are listed in Table II.

The mean-square jitter at the end of a long chain of repeaters is approximately [using (58) and (68)]

$$\overline{\theta_N^2} \approx \frac{\Phi BN}{2} \tag{69}$$

This last approximation can also be derived from direct integration of (9).

APPENDIX D

Growth of Alignment Jitter with Number of Repeaters in Chain

The alignment jitter at the nth repeater is given by (27)

$$\Theta_{aN}(s) = \Theta(s) \frac{1}{(1 + (s/B))^N}, \tag{70}$$

where $\Theta(s)$ is the jitter injected at each repeater.

Equation (70) can be written in the iterative form

$$\Theta_{aN}(s) = \Theta_{a(N-1)}(s) \frac{1}{1 + (s/B)}. \tag{71}$$

In the time domain equation (71) becomes:

$$\theta_{aN}(t) = \int_0^t \theta_{a(N-1)}(t - \tau) B e^{-B\tau} \, d\tau. \tag{72}$$

Then,

$$| \theta_{aN}(t) | \leqq M_{N-1}(1 - e^{-Bt})$$

or

$$| \theta_{aN}(t) | \leqq M_{N-1}, \tag{73}$$

where M_{n-1} is the maximum value of $| \theta_{a(N-1)}(t) |$ on the interval.

Carrying the iteration back to the first repeater, we have

$$| \theta_{aN}(t) | \leqq M_o(1 - e^{-Bt})^N$$

or

$$| \theta_{aN}(t) | \leqq M_o \tag{74}$$

where

$$M_o \geqq | \theta(t) |$$

where $\theta(t)$ is the jitter injected at each repeater.

Equations (73) and (74) state that the maximum alignment jitter does not increase as the number of repeaters grows and is never greater than the maximum jitter injected into each repeater. Since the jitter injected at each repeater is limited by the circuitry to a fraction of a cycle, alignment jitter can never be greater than a fraction of a cycle.

REFERENCES

1. Sunde, E. D., Self-timing Regenerative Repeaters, B.S.T.J., **36**, July, 1957, pp. 891–937.
2. DeLange, O. E., The Timing of High-Speed Regenerative Repeaters, B.S.T.J., **37**, November, 1958, pp. 1455–1486.
3. Bennett, W. R., Statistics of Regenerative Digital Transmission, B.S.T.J., **37**, November, 1958, pp. 1501–1542.
4. Rowe, H. E., Timing in a Long Chain of Regenerative Binary Repeaters, B.S.T.J., **37**, November, 1958, pp. 1543–1598.
5. Aaron, M. R., PCM Transmission in the Exchange Plant, B.S.T.J., **41**, January, 1962, pp. 99–141.
6. Kinariwala, B. K., Timing Errors in a Chain of Regenerative Repeaters, B.S.T.J., **41**, November, 1962, pp. 1796–1797.
7. Mayo, J. S., A Bipolar Repeater for Pulse Code Modulation Signals, B.S.T.J., **41**, January, 1962, pp. 25–97.